Journal of Anatomy

J. Anat. (2009) **214**, pp183–195 doi: 10.1111/j.1469-7580.2008.00986.x

Endothelial CD200 is heterogeneously distributed, regulated and involved in immune cell–endothelium interactions

Ya-Chen Ko,[1,2] Hsiung-Fei Chien,[3] Ya-Fen Jiang-Shieh,[4] Chiu-Yun Chang,[5] Man-Hui Pai,[5] Jian-Pei Huang,[6] Hui-Min Chen[5] and Ching-Hsiang Wu[1]

[1]*Graduate Institute of Life Sciences, National Defense Medical Center, Taipei, Taiwan*
[2]*Department of Radiological Technology, Yuanpei University, Hsinchu, Taiwan*
[3]*Department of Surgery, College of Medicine, National Taiwan University, Taipei, Taiwan*
[4]*Department of Anatomy, National Cheng Kung University Medical College, Tainan, Taiwan*
[5]*Department of Anatomy and Electron Microscopy Center, College of Medicine, Taipei Medical University, Taipei, Taiwan*
[6]*Department of Obstetrics and Gynecology, Mackay Memorial Hospital, Taipei, Taiwan*

Abstract

CD200 is a highly glycosylated cell surface protein containing two immunoglobulin superfamily domains in the extracellular region and performs immunosuppressive activities. It is widely distributed in various tissues including the vascular endothelium. We report here the distribution of CD200 in rat endothelia from different vascular beds. Endothelial CD200 immunoreactivity was weakly expressed in most arteries but was intensely expressed in the arterioles, most veins and venules, as well as continuous and fenestrated capillaries. The distribution of CD200 in the sinusoidal and lymphatic endothelia was variable. Immunoelectron microscopic studies revealed that endothelial CD200 varied considerably not only in different microvasculatures but also in the membrane domains at the subcellular level. Endothelial CD200 expression was differentially regulated by lipopolysaccharide in cell types both *in vivo* and *in vitro*. Functional assessments of endothelial CD200 suggested that the physical binding between CD200 and CD200 receptor (CD200R) was involved in T-cell adhesion to the endothelium but not in macrophage–endothelium interaction. In the latter, however, CD200 agonist, a synthetic peptide from complementarity-determining region 3 of mouse CD200, may trigger CD200R signaling in macrophages to suppress their adhesion to the endothelium. Our findings demonstrate that the distribution, subcellular localization, and lipopolysaccharide-regulation of endothelial CD200 are heterogeneous, and provide evidence elucidating the functional roles of endothelial CD200 during tissue inflammation.

Key words CD200; endothelial cells; heterogeneity; immune cell adhesion; inflammation; lipopolysaccharide; subcellular localization.

Introduction

CD200 (OX-2) is a highly glycosylated membrane protein expressed on the cell surface in various tissues. It contains two immunoglobulin superfamily (IgSF) domains in the N-terminal extracellular region, a transmembrane domain, and a short stretch of a 19-amino acid intracellular tail (Barclay & Ward, 1982; Clark et al. 1985). It is widely distributed in different cell types including neurons, activated T lymphocytes, B lymphocytes, dendritic cells, placental trophoblasts, some smooth muscle cells, and epithelial cells of the hair follicle (McMaster & Williams, 1979; Barclay, 1981; Bukovsky et al. 1983; Webb & Barclay, 1984; Wright et al. 2001; Rosenblum et al. 2004b). CD200 was shown to exert its immunosuppressive and anti-inflammatory activities through interaction with the CD200 receptor (CD200R) (Wright et al. 2000) in murine plasmacytoid dendritic cells, basophils, and mast cells (Fallarino et al. 2004; Cherwinski et al. 2005; Shiratori et al. 2005) and was suggested to contribute to the suppressed immune responses during cellular apoptosis (Rosenblum et al. 2004a). In CD200 null mice, spontaneous activation of macrophage lineage cells and earlier onset of inflammatory diseases in disease models were reported (Hoek et al. 2000). CD200 has now been linked to inhibition of graft rejection, prolonging transplantation survival (Gorczynski et al. 1999), to prevention of spontaneous abortion (Gorczynski et al. 2002), and to protection of inflammation-mediated neurodegeneration (Chitnis et al. 2007), founded on its immunosuppressive activity.

Correspondence
Dr Ching-Hsiang Wu, Department of Biology and Anatomy, National Defense Medical Center, 161, Sec. 6, Min-Chuan East Road, Taipei 114, Taiwan. F: +886 2 87910787; E: microgli@mail.ndmctsgh.edu.tw

Accepted for publication *22 August 2008*

Blood vessels possess structural differences to adapt to local environments and are categorized into arteries, veins, and distinct types of capillaries. In different organs, capillaries fall into several types: continuous non-fenestrated, continuous fenestrated, and discontinuous/sinusoidal capillaries based on the unique features of the endothelium (Aird, 2007). It has been well recognized that endothelial cell heterogeneity exists among different vascular beds (Aird, 2003, 2007; Minami & Aird, 2005). The endothelial cells from arteries, veins, and different capillaries vary in their structures, functions, expression patterns, and signaling pathways. The variations are believed to be acquired from intrinsic cellular characteristics or local environmental cues. For example, surface molecules crucial for leukocyte–endothelial cell interaction such as ICAM-1, VCAM-1, and CD31 have been shown to be differentially expressed among endothelial cells from different sites (Haraldsen et al. 1996; Henninger et al. 1997; Pusztaszeri et al. 2006). Additionally, endothelial cell-derived hemostatic factors such as vWF, tPA, and thrombomodulin also exhibit vascular bed-specific expression (Ishii et al. 1986; Levin et al. 1997; Yamamoto et al. 1998; Pusztaszeri et al. 2006). It is documented that endothelial cell adhesion molecules such as ICAM-1 and VCAM-1 were increased after lipopolysaccharide (LPS) administration. The induction levels of these adhesion molecules were responsible for immune cell–endothelium interaction (Rao et al. 2007) and exhibited heterogeneity in the responsiveness to LPS among different endothelial cell types (Haraldsen et al. 1996; Henninger et al. 1997). These evidences suggest that functional heterogeneity of the vascular endothelium highly correlates with differential surface protein expression and cytokine sensitivity.

Among the endothelial surface molecules, CD200 has been reported to be distributed on the vascular endothelia of the lymph nodes, kidneys, liver, corpora lutea and fallopian tubes (Barclay, 1981; Bukovsky et al. 1983; Wright et al. 2001). The exact roles of endothelial CD200, however, remain to be fully ascertained. It was surmised that a fuller understanding of the expression pattern of CD200 might provide further insight and a better understanding of the functional heterogeneity of endothelium. This study examined the distribution of endothelial CD200 in different types of blood vessels including capillaries and lymphatic vessels. Subcellular localization of endothelial CD200 was also examined by immunoelectron microscopy. Furthermore, CD200 expression in different endothelia under septic challenge was also investigated. The possible roles of endothelial CD200 in immune cell–endothelium interactions were also assessed.

Materials and methods

Animal procedure and tissue processing

Adult Wistar rats weighing 300–350 g were used in this study. They were anesthetized with a single intraperitoneal injection of 7% chloral hydrate (0.4 mL 100 g^{-1} body weight; Sigma, C-8383). Following anesthesia, the rats were given an intravenous injection of 100 $\mu g\ kg^{-1}$ LPS (Sigma; LPS from *Escherichia coli*, serotype O55:B5, L-2880) or the same volume of normal saline alone. After 48 h, the rats were sacrificed by intracardiac perfusion each with 100 mL normal saline followed by a fixative containing 4% paraformaldehyde in 0.1 M phosphate buffer (PB), pH 7.4. Tissue samples containing different types of endothelia in the heart, skeletal muscle, kidney, vas deferens, liver, spleen, bone marrow, cerebellum, pineal, salivary glands and lymph node were removed, immersed in 30% sucrose in 0.1 M PB overnight at room temperature, and cryosectioned at 10 μm thickness.

Immunohistochemistry

Tissue sections were mounted on gelatin-coated slides. After washing with 0.05 M Tris-buffered saline (TBS), pH 7.4, the sections were treated with 1% H_2O_2 for 30 min, incubated in 2% normal goat serum (Nalgene, 2939149) for 1 h, followed by anti-rat CD200 monoclonal antibody (Serotec, MCA44G) with a dilution of 1 : 100 in TBS containing 0.1% Triton X-100 overnight at room temperature. Immunostaining was visualized by detection of peroxidase activity or fluorescence. For peroxidase activity detection, tissue sections were further incubated with biotinylated horse anti-mouse IgG (1 : 300; Vector, BA-2001) for 1 h at room temperature, peroxidase-conjugated streptavidin (1 : 300; Dako Cytomation, P0397) for 1 h at room temperature, and 0.025% 3,3′-diaminobenzidine tetrahydrochloride hydrate (DAB; Sigma, D5637) in 0.02% H_2O_2 for up to 15 min. The stained sections were examined and photographed under a Zeiss Axiophot microscope. For sinusoidal endothelial CD200 fluorescence detection, tissue sections were further incubated with FITC-conjugated donkey anti-mouse IgG (1 : 300; Jackson ImmunoResearch Laboratories, 715-095-150) for 2 h at room temperature. Cell nuclei were stained with TOTO-3 iodide (1 : 10 000; Molecular Probes, T3604) for 5 min at room temperature. Sections were then examined and photographed under a Zeiss LSM 510 confocal microscope.

Double fluorescence labeling

Tissue sections were first blocked and permeabilized with 2% normal goat serum/0.1% Triton X-100 for 1 h at room temperature. After blocking, the sections were incubated with anti-rat CD200 monoclonal antibody (Serotec, MCA44G) and anti-podoplanin antibody (Sigma, P1995) in 0.05 M TBS containing 0.1% Triton X-100 overnight at room temperature. Subsequent antibody detection was carried out using FITC-conjugated goat anti-rabbit IgG (1 : 300; Sigma, F9887) and cyanine dye 5 (Cy5)-conjugated goat anti-mouse IgG (1:300; Jackson ImmunoResearch Laboratories, 115-175-166) for 1.5 h. The sections were then examined and photographed under a Zeiss LSM 510 confocal microscope.

Immunoelectron microscopy

The tissues were sectioned into 50-μm-thick slices using a vibratome. Sections were incubated with anti-rat CD200 monoclonal antibody for immunoelectron microscopy as for light microscopy with the substitution of 0.01% Triton X-100 used in the solution. All sections were then rinsed in 0.1 M PB, pH 7.4, post-fixed with 1% OsO_4 dissolved in PB, dehydrated with alcohol, and embedded

in Epon-Araldite mixture. Ultra-thin sections were obtained using a diamond knife. Tissue sections were examined and photographed under a Hitachi 600 electron microscope attached with a CCD camera.

Cell culture and endotoxin treatment

Human umbilical vein endothelial cells (HUVECs) were isolated from fresh human umbilical cords by collagenase digestion method and maintained in Medium 199 (Gibco) supplemented with 20% fetal bovine serum (FBS, Biological Industries Kibbutz Beit Haemek, Israel) and 100 U mL^{-1} penicillin/streptomycin (Biological Industries Kibbutz Beit Haemek). Cells of secondary passage were used for experiments. Human aortic endothelial cells (HAECs) were a generous gift from Dr Yuh-Lien Chen, Department of Anatomy and Cell Biology, College of Medicine, National Taiwan University. HAECs were maintained in Medium 200 (Cascade Biologics) supplemented with Low Serum Growth Supplement (Cascade Biologics) and 100 U mL^{-1} penicillin/streptomycin. Human microvascular endothelial cells isolated from adult dermis (HMVECs) were purchased from Cascade Biologics and maintained in Medium 131 (Cascade Biologics) supplemented with Microvascular Growth Supplement (Cascade Biologics) and 100 U mL^{-1} penicillin/streptomycin. Human brain microvascular endothelial cells (HBMECs) were purchased from ScienCell™ Research Laboratories and maintained in Endothelial Cell Medium (ScienCell™ Research Laboratories). Mouse brain endothelial cell line bEnd.3, mouse pancreatic endothelial cell line SVR, and monocyte/macrophage cell line RAW 264.7 were maintained in Dulbecco's Modified Eagle's Medium with D-glucose 4500 mg L^{-1} and glutamine (DMEM, Biological Industries Kibbutz Beit Haemek) supplemented with 10% FBS and 100 U mL^{-1} penicillin/streptomycin. Human T lymphocyte cell line (Jurkat T cell) was maintained in RPMI 1640 medium containing L-glutamine (Gibco) supplemented with 10% FBS and 100 U mL^{-1} penicillin/streptomycin. All cells were kept in a humidified incubator with 5% CO_2 at 37 °C. Endothelial cells were plated on 35-mm culture dishes until confluence and stimulated with LPS in the growth medium.

RNA extraction and reverse transcription-polymerase chain reaction (RT-PCR) analysis

Total RNAs from endothelial cells, Jurkat T cells, or RAW 264.7 cells pre-incubated with CDR3 peptides were extracted using Trizol® Reagent (Invitrogen) according to the manufacturer's instructions. cDNA was synthesized using StrataScript® First-Strand Synthesis System (Stratagene). For PCR, the primers including human CD200, ICAM-1, β-actin and others were used (Table 1).

Flow cytometry

Surface expression of CD200 and CD200R1 on bEND.3, RAW 264.7, SVR, and HMVECs were analyzed with antibodies against mouse CD200 (Serotec, MCA1958XZ), mouse CD200R1 (R&D Systems, MAB2554), human CD200 (Serotec, MCA1960XZ), and the isotype-matched rat IgG2a (BD Pharmingen, 553927) and mouse IgG1 (eBioscience, 14-4714). Cells (5×10^5) were incubated with the primary antibodies or the isotype-matched IgG for 2 h at 4 °C and then washed twice with 4% bovine serum albumin (BSA) in phosphate-buffered saline (PBS). After the cells were incubated with R-phycoerythrin (RPE)-conjugated goat anti-rat IgG (AbD Serotec, STAR73) or FITC-conjugated goat anti-mouse IgG (Sigma, F9006) for 1 h at 4 °C, cells were washed twice with 4% BSA in PBS, fixed with 4% paraformaldehyde in 0.1 M PB, and then analyzed by flow cytometry on a FACS Calibur™ (BD Biosciences).

Table 1 Sequences of the primers used for PCR in the present study

Gene	Sequence (5′ to 3′)
human CD200	AAGGATGGAGAGGCTGGTGA
	GCTCTCGGTCCTGATTCCGG
human CD200R1	CTTCCTGTTCCAGGTGCCAAA
	GCCTCAGATGCCTTCACCTTG
human ICAM-1	CAGTGACCATCTACAGCTTTCCGG
	GCTGCTACCACAGTGATGATGACAA
human β-actin	CACCCCGTGCTGCTGACCGAGGCC
	CCACACGGAGTACTTGCGCTCAGG
mouse CD200	AGTGGTGACCCAGGATGAA
	TACTATGGGCTGTACATAG
mouse ICAM-1	CAGATGCCGACCCAGGAGAG
	ACAGACTTCACCACCCCGATG
mouse ITGA4	TGCGGAAGCGAGGTGCAGAC
	CTTTCTGATCCCGCATCTGT
mouse ITGB2	TTGCCCTAGCTGGACTGTTC
	GGCTGGACAACCCTTCAGCA
mouse PSGL-1	TAGAGAGAGATTCCACGAGC
	AGGTTCTGTGGAAGGGACTT
mouse β-actin	TCCTTCGTTGCCGGTCCACA
	CGTCTCCGGAGTCCATCACA
mouse GAPDH	TGGCAAAGTGGAGATTGTTGCC
	AAGATGGTGATGGGCTTCCCG

Cell adhesion assay

Endothelial cells were seeded on 24-well culture plates and grown until confluence. Before adhesion assay, the endothelial cell monolayer was checked for confluency and integrity under an inverted light microscope. RAW 264.7 or Jurkat T cells were first stained with CellTracker™ Red CMTPX dye (Molecular Probes) according to the manufacturer's protocol. After staining, RAW 264.7 cells were pre-incubated with either 50 μg mL^{-1} of CDR3 peptide (CLFNTFGSQKVSGTA) or the same volume of PBS for 1 h at room temperature. The CDR3 peptide is synthesized according to the complementarity-determining region 3 of the NH_2-terminal of mouse CD200 molecule. This peptide has been shown to abrogate the immunosuppressive effect of CD200 in mixed leukocyte culture reactions (Chen et al. 2005). The endothelial cells were incubated with either anti-CD200 antibody or isotype-matched IgG at the same concentration of 80 μg mL^{-1} for 1 h at 37 °C. RAW 264.7 cells or Jurkat T cells (1×10^6 cells per well) were then added onto the endothelial cell monolayer for adhesion at 37 °C. After 40 min, non-adhered cells were gently washed away twice by pre-warmed PBS. The attached fluorescent cells were photographed using a Zeiss LSM 510 confocal microscope. For quantification, fluorescence intensities in the wells were measured by an automatic microplate fluorometer Fluoroskan Ascent FL (Thermo Scientific). RAW 264.7 cells pre-incubated with CDR3 peptides (50 μg mL^{-1}) for various time points were also analyzed to determine the possible changes of adhesion molecule expression by RT-PCR.

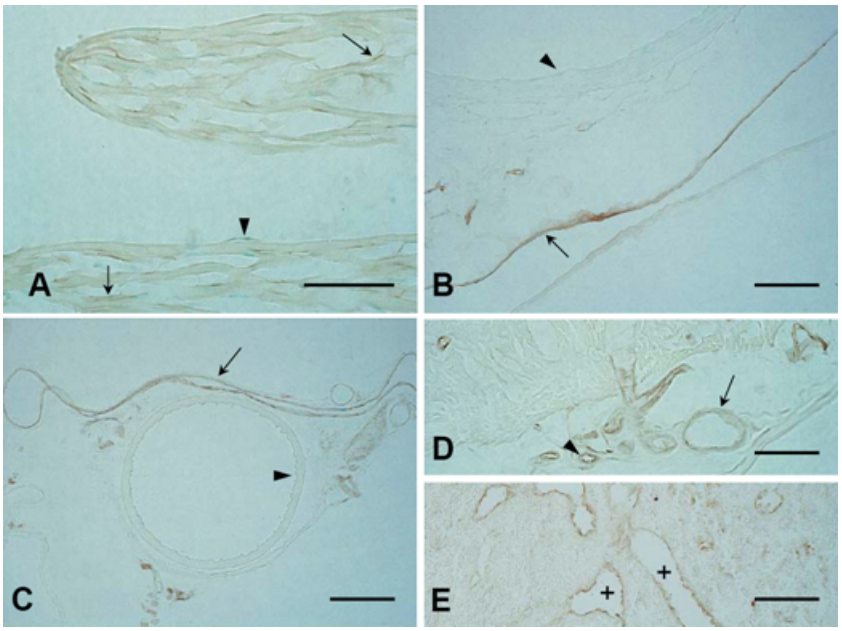

Fig. 1 CD200 distribution at the endothelia in different vascular regions in rats. CD200 monoclonal antibody marks capillaries (A, arrow) between the cardiac muscle cells but not the endothelial cells (A, arrowhead) along the endocardium of the heart. Intense CD200 is also detected at the endothelia of large veins such as the inferior vena cava (B, arrow) but not those of the aortic wall (B, arrowhead). The small artery (C, arrowhead) and accompanying vein (C, arrow), e.g. lumbar artery and vein, show a similar distribution pattern to CD200. CD200 is detected both on the endothelia of the arteriole (D, arrowhead) and venule (D, arrow). The specialized venules with high endothelia (E, +) in the lymph node also exhibit intense CD200 immunostaining. Scale bars = 50 μm.

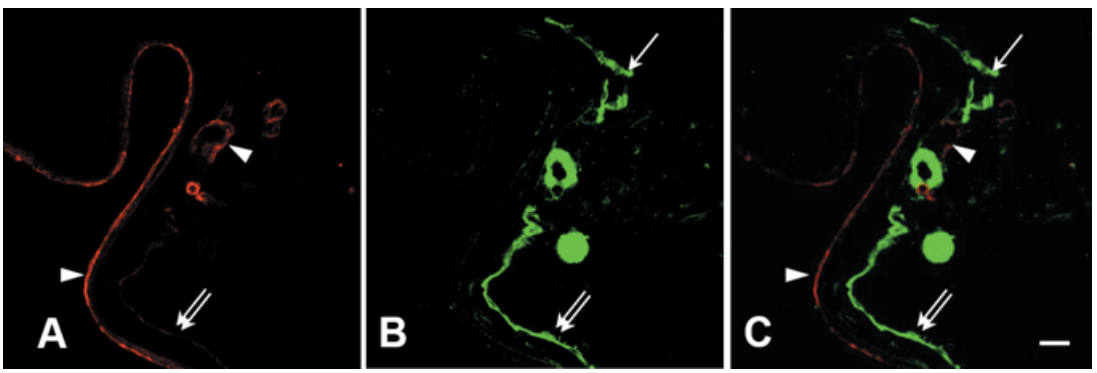

Fig. 2 Confocal microscopy images of CD200 and podoplanin on the lymphatic vessels in rat mammary gland. CD200 (red) is localized at the endothelia of veins (A,C, arrowheads). Podoplanin (green), a specific marker of lymphatic endothelia, outlines the adjacent lymphatic vessels that express either weak (A–C, double arrows) or undetectable (A–C, arrow) CD200. Scale bar = 20 μm.

Statistical analysis

All quantitative data were given as mean ± SD from experiments each done in triplicate. Data were analyzed using Student's *t*-test. The data were considered statistically significant if $P < 0.05$.

Results

CD200 distribution on the endothelium along the vascular tree

The distribution of endothelial CD200 was examined by immunohistochemistry staining with a monoclonal CD200 antibody on various tissues of normal rats. Expression of endothelial CD200 varied among different endothelia along the vascular tree (Fig. 1). Endothelia of the large veins, small veins, and venules (Fig. 1B–D) showed intense CD200 immunoreactivity. The specialized endothelium of the high endothelial venule (HEV) in the lymph node exhibited pronounced CD200 immunoreactivity (Fig. 1E). In the arterial endothelium, however, CD200 immunoreactivity was barely detected in larger vessels including the aorta and small artery (Fig. 1B,C). This is also true in the cardiac endothelium (Fig. 1A). The intensity of endothelial CD200 staining appeared to increase with reduced arterial diameter (Fig. 1B–D).

Although the lymphatic endothelium is considered to be derived from venous sprouting (Alitalo & Carmeliet, 2002), it possesses a different morphology and surface markers from the vascular endothelium. To investigate the presence of CD200 in the lymphatic endothelium, rat tissue sections were labeled with antibodies against CD200 and the lymphatic endothelial marker podoplanin. Immunofluorescence double labeling confirmed that the expression of CD200 on the lymphatic endothelium was rather limited (Fig. 2). In the rat mammary gland, podoplanin-positive lymphatic vessels displayed either a very moderate expression

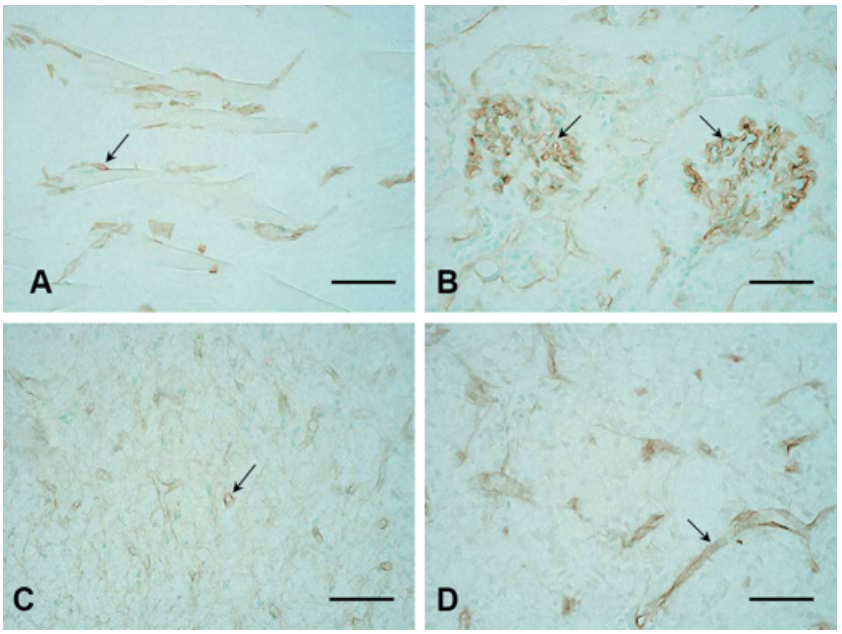

Fig. 3 CD200 distribution in different microvascular endothelia of rats. Almost all endothelia in the microvasculature express CD200. CD200 immunostaining is detected in endothelia of the continuous non-fenestrated type capillaries in the skeletal muscle (A, arrow), and the cerebellar white matter with blood-brain barrier (C, arrow). CD200 is conspicuous at endothelia of the continuous fenestrated type capillaries in the renal glomeruli (B, arrows) and the pineal gland (D, arrow). Scale bars = 50 μm.

of CD200 or lack of it when compared with the adjacent CD200-enriched venous endothelium (Fig. 2A–C).

CD200 distribution in different types of capillaries

Distribution of endothelial CD200 in the capillaries was carefully examined by immunohistochemistry, which revealed that it differed among distinct types of capillaries characterized by their structure and permeability. CD200 immunoexpression was intense in the continuous non-fenestrated (Figs 1A, 3A,C) and continuous fenestrated (Fig. 3B,D) endothelia. In the spleen, endothelial CD200 immunoreactivity was unevenly distributed. It was hardly detected in the white pulp and appeared to vary considerably in different regions of the red pulp venous sinuses. Relatively intense CD200 staining, however, was seen in the region surrounding the white pulp, corresponding to the location of the marginal sinuses, as well as the endothelium of the central artery (Fig. 4A,B). Interestingly, in the liver, CD200 immunoreactivity was barely detected in the endothelia of sinusoids (discontinuous endothelium) and the central veins, and very weak CD200 immunoreactivity was observed in the portal venules and hepatic arteries within the hepatic triads (Fig. 4C). Sinusoidal endothelium of bone marrow was weakly immunoreactive in a diffused manner (Fig. 4D).

Subcellular localization of CD200 in the microvascular endothelial cells

Subcellular localization of endothelial CD200 in different types of capillaries was further examined by immunoelectron microscopy. CD200 immunoreactivity was generally detected on the plasma membrane of endothelial cells. Capillaries in the central nervous system showed a diverse staining pattern. In the hippocampus endowed with blood-brain barrier (BBB), a unique CD200 localization was observed in which only the luminal surface of the endothelial cells was stained (Fig. 5A). In the area postrema representing the CNS non-BBB region, CD200 was detected on both the luminal and the abluminal surfaces of the endothelial cells in the fenestrated capillaries (Fig. 5B). In the salivary glands, a more complex subcellular localization of CD200 was observed. In the capillaries of the submandibular gland, CD200 was differentially distributed within the endothelium. It was localized either on the luminal surface (Fig. 6A) or on both surfaces of the endothelial cells (Fig. 6B). The non-barrier-forming endothelia showed significant differences in their variable distributions of CD200 in both surfaces of cells and discernible expression in numerous caveolae and cytoplasmic vesicles when compared with those bearing BBB. A similar distribution pattern of endothelial CD200 was also found in the parotid gland, which displayed an uneven CD200 staining on endothelial cells lining one specific vessel lumen, where CD200 immunoreactivity was either positive or negative on different endothelial microvilli and patches of the plasma membrane (Fig. 6C,D).

Heterogeneous expression of CD200 is found not only among different endothelia but also within one individual endothelial cell. In the capillaries around the lung alveoli, endothelial CD200 was distributed only on the luminal plasma membrane along the thin portion of the alveolar septum constituting the blood-air barrier but not the thick portion, where the endothelial cell was in contact with a larger amount of stromal connective tissue or cells (Fig. 7A). A weaker CD200 immunoreactivity was also detected in the plasma membrane region where the

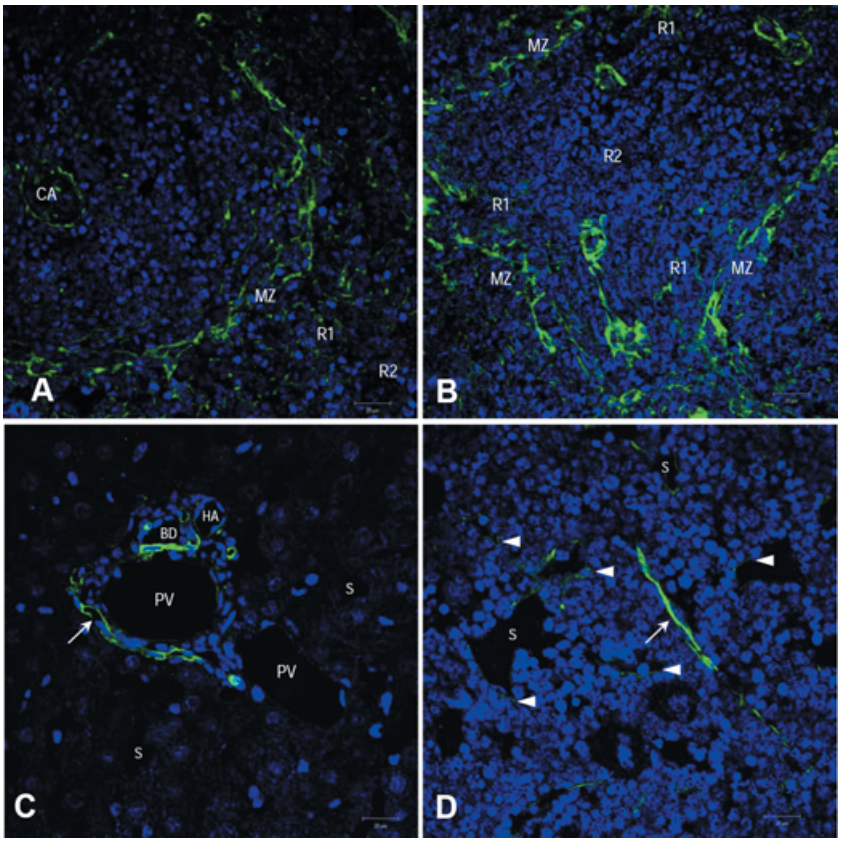

Fig. 4 CD200 expression in organs containing sinusoidal endothelia. In the splenic microvasculature (A,B), sinusoidal endothelia show intense CD200 expression in the marginal zone (MZ); a moderate expression is seen in the adjacent red pulp (R1). In areas further from the marginal zone (R2), CD200 expression is weak or absent. CD200 expression is absent in the endothelia of liver venous sinusoid (C, S), while endothelial cells in the hepatic triad are CD200-positive (C, arrow). CD200-positive sinusoids are observed in the bone marrow (D, S) with a weak and patchy expression pattern (D, arrowheads). This is in contrast to an intense CD200 expression in the capillary (D, arrow). CA, central artery; PV, portal vein; BD, bile duct; HA, hepatic artery. Scale bars = 20 μm.

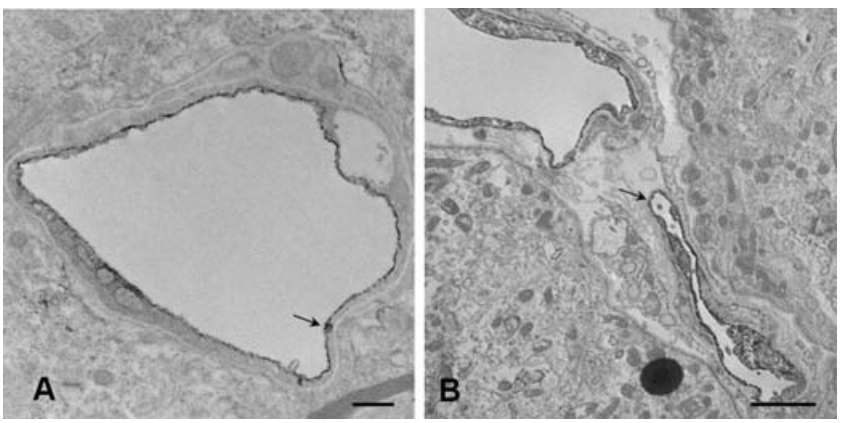

Fig. 5 Subcellular localization of endothelial CD200 in the rat nerve microvasculatures with or without BBB. In the hippocampus (A), microvascular endothelial cell possesses BBB and shows CD200 immunoreactive product on its luminal front and sporadic vesicles in the endothelial cytoplasm (arrow). The fenestrated and non-BBB endothelia in area postrema (B) express intense CD200 immunoreactivity on their luminal and abluminal (arrow) surfaces. Scale bar: A = 500 nm, B = 2 μm.

endothelial cell was bulging with its nucleus and abundant cytoplasm (Fig. 7B).

Differential regulation of CD200 expression by LPS in the macrovascular and microvascular endothelial cells

As CD200 is involved in immunosuppressive activity during tissue inflammation, it prompted us to question whether endothelial CD200 expression is regulated by the pro-inflammatory agent LPS. Rats were injected intravenously with either LPS or normal saline and frozen sections of tissues were subjected to CD200 immunostaining. In the macrovasculatures, CD200 immunoreactivity was very weak on the arterial endothelium of saline-injected rats but was more intense after LPS administration. CD200 immunoreactivity remained high in the accompanying veins and was comparable between the control and LPS-treated groups (Fig. 8A,B). Further evaluation of the effect of LPS was performed *in vitro*. Human macrovascular and microvascular endothelial cells were cultured and the mRNA expression levels were examined by RT-PCR analyses. In HUVECs, a significant amount of CD200 mRNA expression was induced after 4 h followed by a slight rise after 12 h of LPS treatment (Fig. 8C). The effect of 4-h LPS treatment on CD200

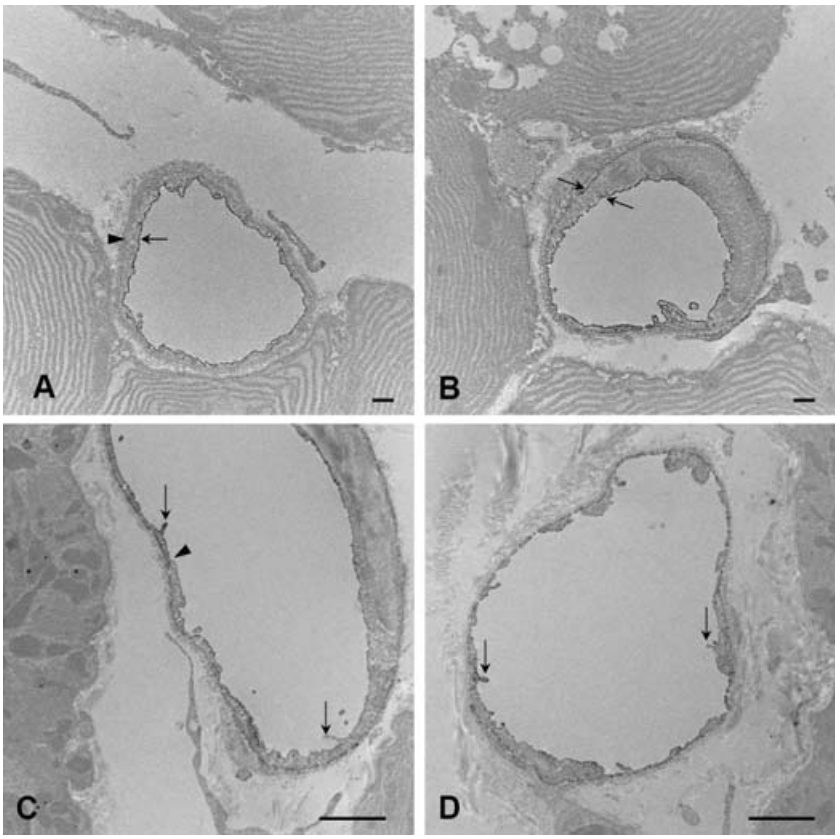

Fig. 6 Diverse subcellular distribution and expression of CD200 on microvascular endothelia in the salivary glands of rats. In the submandibular gland, the abluminal surface (A, arrowhead) of some capillary endothelia lacks CD200, whereas the luminal surface exhibits intense labeling (A, arrow). Some capillaries in the same gland, however, show CD200 immunoreactivity both on the luminal and abluminal surfaces (B, arrows) of endothelia. In the parotid gland (C,D), CD200 immunoreactivity is intense in some areas of the endothelial cell membrane regardless of endothelial type. A striking feature is the localization of intense CD200 staining on some endothelial microvilli (C,D, arrows) and at the endothelial junctions (C, arrowhead). Scale bars: A, B = 500 nm; C, D = 2 μm.

expression in HUVECs was dose-dependent, reaching a plateau at the LPS concentration of 0.01 μg mL^{-1} (Fig. 8G). In HAECs, CD200 expression was increased after 2–4 h of LPS treatment (Fig. 8D). In two types of endothelial cells derived from the human microvasculature, HMVECs of adult dermis and HBMECs of the brain, CD200 mRNA expression levels remained high and were not altered by LPS at the time points examined (Fig. 8E,F). Endothelial cell lines derived from different mouse microvasculatures such as bEND.3 from the brain and SVR from the pancreas were further examined. The results again supported the concept of endothelial heterogeneity in response to LPS stimulation that no significant change on CD200 expression was observed in the CD200-rich bEND.3 cells (Fig. 8H), but significant up-regulation of CD200 expression was detected in the CD200-absent SVR cells (Fig. 8I).

Role of CD200 in the immune cell–endothelium interaction

Cell surface proteins with IgSF domains mainly function as recognition molecules mediating cell–cell and cell–matrix interactions notably influenced by bacterial endotoxin, which has been shown to up-regulate endothelial CD200 expression in our studies. Involvement of endothelial CD200 in the cell–cell interactions between immune cells and the endothelium has not been documented and was therefore investigated. The presence of CD200 on bEND.3 and CD200R (CD200R1) on the mouse macrophage cell line RAW 264.7 was confirmed by flow cytometric analysis (Fig. 9A). Adhesion of RAW 264.7 to bEND.3 was assessed by quantifying fluorescence-labeled macrophages settled on the endothelial cell monolayer. In the control group, RAW 264.7 macrophages were able to adhere on bEND.3 monolayer after 40 min of contact. The adhesion was not significantly affected by pre-incubation of bEND.3 monolayer with anti-CD200 antibody (Fig. 9B). Interestingly, the cell population of adhered macrophages was significantly attenuated by pre-incubating macrophages with the synthesized CDR3 peptide (Fig. 9B), which consists of 15 amino acids lying within the extracellular portion of CD200 and has been validated as capable of interrupting the interaction between CD200 and CD200R1 (Chen et al. 2005). The results suggested that the decreased adhesion is due to the CDR3-triggered CD200R1 immunosuppressive signaling to down-regulate the macrophage adhesion ability on endothelial cells but not the blockage of CD200-CD200R1 physical binding. To further evaluate the CDR3 effect on macrophages, adhesion of RAW 264.7 on a CD200-negative (Fig. 9A) mouse endothelial cell line SVR was assessed (Fig. 9C). CDR3 was, as expected, able to inhibit macrophage adhesion in the absence of endothelial CD200. To delineate the underlying mechanisms of CDR3-mediated inhibition of macrophage adhesion, expression patterns of

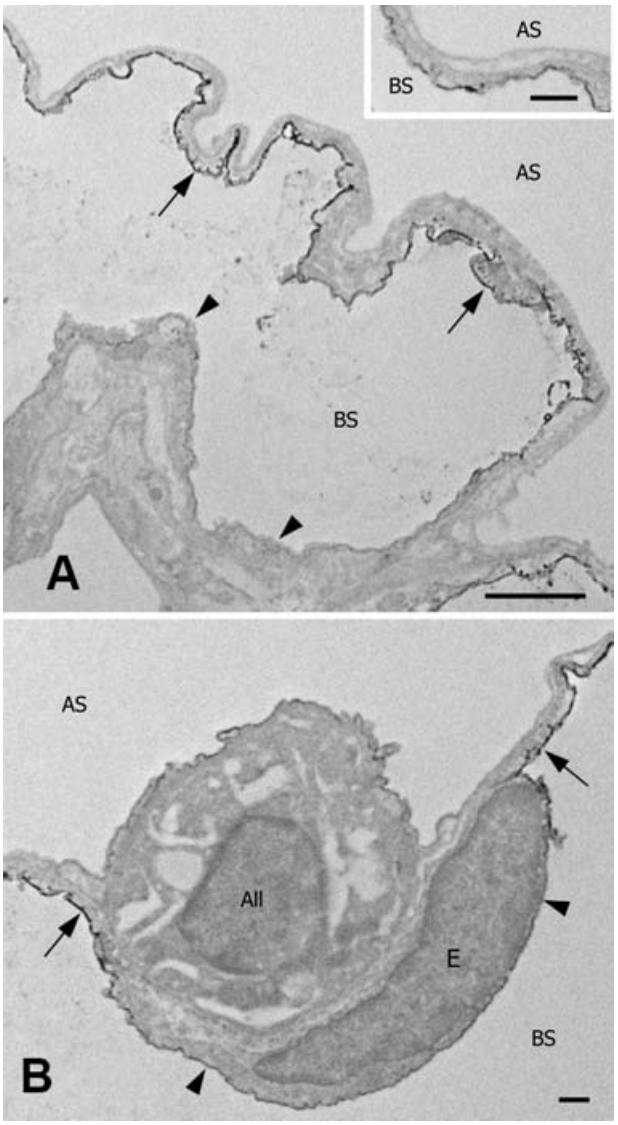

Fig. 7 Differential CD200 expression on the alveolar endothelia of the lungs. Note that endothelial CD200 immunoreactivity on the luminal surface of the pulmonary capillary is intense along the thin portion (A,B, arrows) but very weak along the thick portion (A, arrowheads) of the alveolar sac. A weaker endothelial CD200 immunoreactivity is seen on the luminal membrane (B, arrowheads) where the alveolar septum is thickened with the endothelial nucleus (B,E) and type II alveolar epithelial cell (B, AII). The inset in A shows a high magnification of a portion of the alveolar septum. BS, blood space; AS, air space; Scale bars: A = 2 μm; inset, B = 500 nm.

selected macrophage adhesion molecules on RAW 264.7 were then analyzed by RT-PCR. The present analysis showed that mRNA expressions of macrophages integrin α4 (ITGA4) and ICAM-1 were decreased after incubation with CDR3, whereas those of integrin β2 (ITGB2) and P-selectin glycoprotein ligand-1 (PSGL-1) were unaltered (Fig. 9D).

Considering that the neutralization effect of anti-CD200 antibody used in the present study is possibly cell type-specific and therefore ineffective in blocking RAW 264.7 adhesion on bEND.3 monolayer, adhesion of a human T lymphocyte cell line (Jurkat T cells) on HMVECs was then evaluated with the same type of antibody treatment. Constitutive CD200 and CD200R (CD200R1) expression in the respective HMVECs and Jurkat T cells was initially verified (Fig. 10A,B). CD200 antibody treatment revealed that the adhesion of Jurkat T cells on the HMVEC monolayer was partially blocked by the antibody pre-incubation with the endothelial cells (Fig. 10C,D). Our results suggest that CD200-CD200R1 physical binding contributes to the T cell adhesion on the endothelium to a certain extent but does not play a pronounced role in the macrophage–endothelium interaction.

Discussion

Heterogeneous distribution of endothelial CD200

This study has demonstrated that the distribution of endothelial CD200 *in vivo* is heterogeneous among different sites of the vascular beds. CD200 is mainly expressed in the endothelia of veins, venules, arterioles, continuous and fenestrated capillaries, as well as sinusoidal capillaries in the bone marrow and the spleen, whereas it is barely observed in the endothelia of large arteries, sinusoids and central veins of the liver and lymphatic vessels. The observation is consistent with previous reports (Barclay, 1981; Wright et al. 2001) and extends further to a complete examination of various endothelial regions in the vascular system. Apart from CD200, it is well known that a large number of endothelial cell genes are heterogeneously expressed in a vessel type-specific or organ-specific manner (Aird, 2003; Chi et al. 2003). Among different vascular sites, the heterogeneity of CD200 expression in endothelial cell subgroups is due to the presence of different intrinsic identities or extrinsic cues from local environments such as blood oxygen pressure, hemodynamic forces, or factors derived from the adjacent tissues. Regarding the extrinsic influences, blood oxygen pressure is unlikely to be a factor as we found that endothelial CD200 expression was very low in the pulmonary artery and high in the pulmonary vein (unpublished observation), which coincided with observation of the systemic circulation. When the gene expression profiles were searched for in the NCBI Gene Expression Omnibus websites, results from microarray studies indicated that hemodynamic forces were likely to regulate expression of genes including CD200 in HUVECs (accession number: GSE1518). Other data further revealed that both high shear stress and high intraluminal pressure were able to decrease CD200 mRNA expression (Andersson et al. 2005). This evidence may partly explain why the arterial endothelium bears less CD200 than its venous counterpart. Interestingly, the presence of CD200 in different discontinuous sinusoidal endothelia is rather

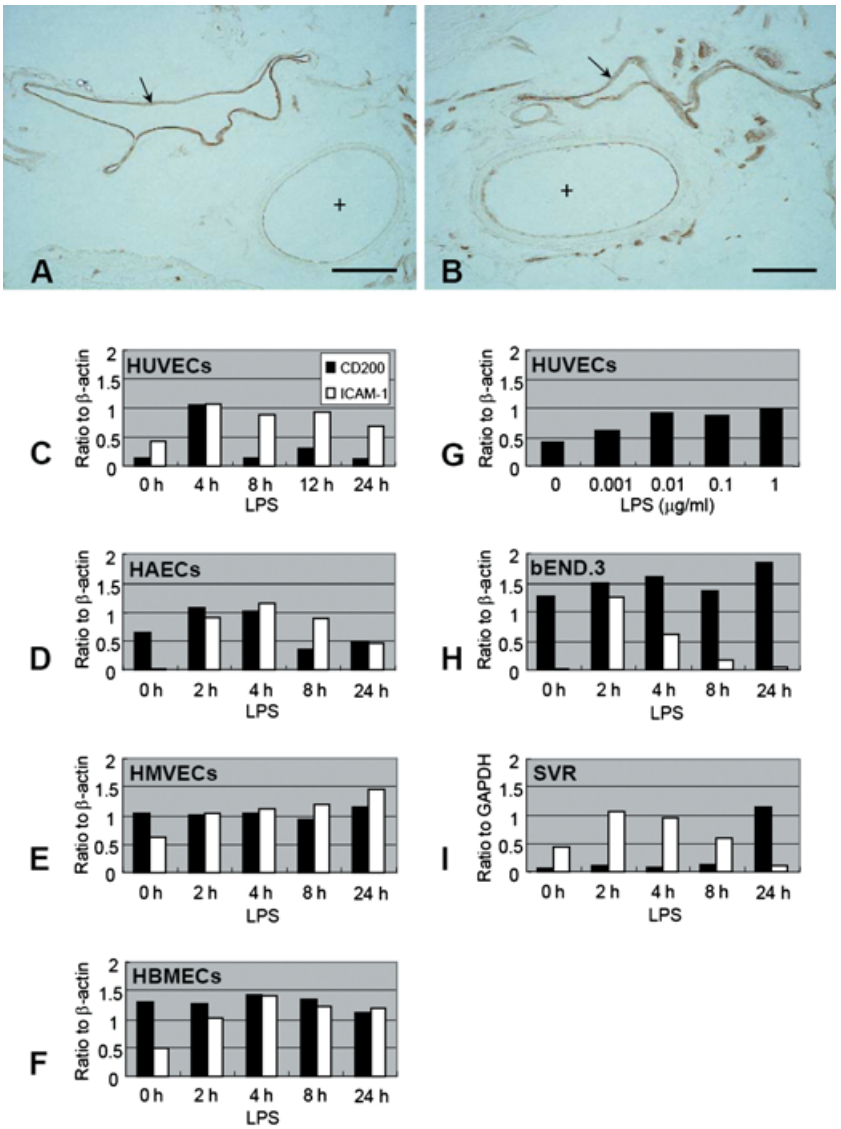

Fig. 8 Effects of LPS on endothelial CD200 expression. CD200 immunohistochemical staining of blood vessels (near the vas deferens) shows that CD200 immunoreactivity is low on the arterial endothelia (A, +) under normal condition but is increased after LPS stimulation (B, +). CD200 expression remains intense on the endothelia of the accompanying veins. The immunoreactivity between the normal (A, arrow) and LPS-challenged conditions is comparable (B, arrow). RT-PCR analysis shows the LPS-regulated CD200 mRNA expression in the endothelia of large vessels, e.g. HUVECs (C) and HAECs (D), is time-dependent. In the former cells, LPS regulates endothelial CD200 mRNA expression in a dose-dependent manner (G). The expression of CD200 mRNA is not altered in microvascular endothelial cell lines such as HMVECs (E), HBMECs (F), and bEND.3 cells (H). In other microvascular endothelial SVR cells, endotoxin exerts a delayed induction on CD200 mRNA expression (I). ICAM-1 mRNA induction is examined to verify the effectiveness of LPS stimulation with that of beta-actin or GAPDH as the loading controls.
Scale bars = 50 μm.

diverse. The staining of CD200 appeared substantial in the marginal zone of the spleen and diffused in the bone marrow, yet it is nearly undetectable in the liver. Therefore, besides the possible contribution of hemodynamic forces, other factors may participate in the regulation.

Immunoelectron microscopic examination revealed that the subcellular localization of endothelial CD200 in the microvasculature also exhibited heterogeneity in terms of its presence on the luminal and/or the abluminal surfaces of the endothelial cells. We have also provided the first evidence demonstrating the uneven distribution of CD200 on the plasma membrane within one individual endothelial cell surrounding the alveolar capillary of the blood-air barrier. This unique expression pattern of CD200 in the pulmonary capillary may be a consequence of the interaction between CD200 and the endothelial cytoskeleton or the basement membrane components and epithelial cells which direct CD200 to locate in a confined membrane domain. Such a configuration may facilitate the immune cell contact to exert its immunoregulatory activity in the lungs. The present findings have demonstrated the complex heterogeneity of endothelial CD200 localization pointing to its multifunctional roles.

Endothelial CD200 may deliver an inhibitory signal for immune cell adhesion

Interactions between immune cells and the endothelium are crucial for the onset of innate immunity, in which the cell surface molecules assist cell–cell adhesion and trigger immunomodulatory signaling between cells. In the present study, failure of anti-CD200 antibody to block macrophage adhesion on the endothelial cells may be attributed to the effort of other major adhesion molecules at the same time. However, addition of CDR3 peptide of CD200 resulted in a decreased adhesion between the two cell types. In the

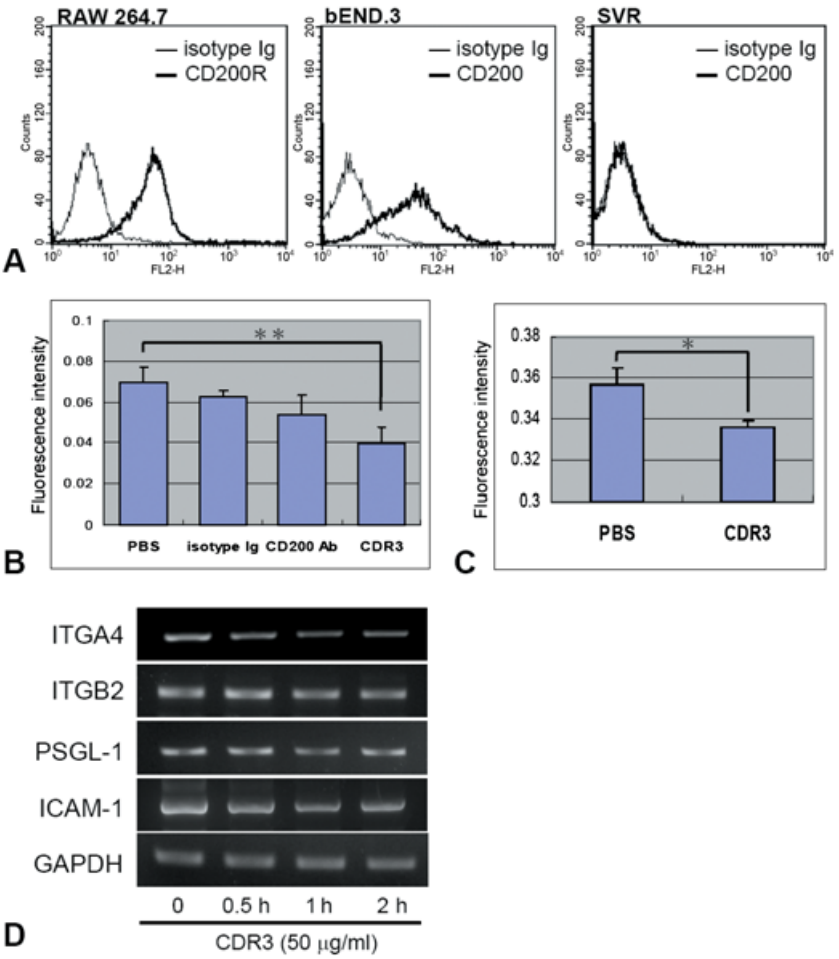

Fig. 9 Involvement of CD200–CD200R1 interaction in mouse macrophage adhesion on endothelial cell lines. Surface expression of CD200 or CD200R (CD200R1) on RAW 264.7, bEND.3, and SVR cells is examined by flow cytometry (A). The data show RAW 264.7 and bEND.3 cells express CD200R1 and CD200, respectively. SVR cells are CD200-negative. Effects of CD200 antibody and CDR3 peptide (CD200 analog) on RAW 264.7 adhesion to bEND.3 monolayers were evaluated by cell adhesion assays (B). The results show evidence of an inhibitory effect of CDR3 peptide on RAW 264.7 adhesion to bEND.3 cells and lack of effectiveness of CD200 antibody and its isotype-matched IgG on the adhesion. Furthermore, CDR3 peptide also inhibits RAW 264.7 adhesion to SVR monolayers that do not express CD200 (C). The results are expressed as mean ± SD. $*P = 0.017$; $**P = 0.009$. RT-PCR analysis of CDR3 peptide-pre-incubated RAW 264.7 cells further reveals that the peptide down-regulates mRNA expressions of ITGA4 and ICAM-1 but not ITGB2 and PSGL-1 in the treated macrophages (D).

mixed leukocyte culture (MLC), administration of CDR3 and other CDR peptides of CD200 significantly blocked the inhibitory effect of CD200-Fc on the production of cytotoxic T lymphocytes (CTLs) and TNF-α (Chen et al. 2005). This report confirmed that CDR3 peptide was capable of blocking the CD200–CD200R1 interaction. It is conceivable that in our experiments, synthetic CDR3 peptide binds to macrophage CD200 receptor to trigger an immunosuppressive signal which down-regulates either quantity or functional activities of macrophage adhesion molecules required for adhesion to endothelial cells. Indeed, the present data evidenced a lower mRNA expression of adhesion molecules (ITGA4 and ICAM-1) in RAW 264.7 macrophages treated with CDR3 peptide. We therefore propose that constitutively expressed CD200 on mouse endothelium acts primarily as a signaling ligand to inhibit macrophage functions. This notion is further supported by the CDR3 inhibition of RAW 264.7 adhesion on the CD200-negative SVR cells. However, we cannot rule out the possibility that CDR3 peptide disrupted the adhesion between bEND.3 and RAW 264.7, by blocking CD200–CD200R1 physical binding.

By examining the interaction between human T cells (Jurkat T cells) and endothelial cells (HMVECs), we found that the adhesion was blocked by anti-human CD200 antibody. It has been reported that different combinations of surface molecules are responsible for trafficking of T cells, monocytes/macrophages, and other leukocytes on the endothelium during tissue inflammation (Miyasaka & Tanaka, 2004; Luster et al. 2005). Thus, CD200–CD200R1 physical binding may play a more prominent role on T cell adhesion than on macrophage–endothelium interaction. Current results together with the pronounced endothelial CD200 expression found in high endothelial venules point out the possibility that CD200–CD200R1 interaction may be involved in the regulation of T lymphocytes' entrance into lymph nodes and Peyer's patches. Different demands of CD200 for immune cell adhesion and availabilities of endothelial CD200 in the blood vessels may contribute to the unequal predisposition of inflammatory pathological conditions such as atherosclerosis and vascular dysfunction during sepsis.

Endothelial CD200 is a cell type-specific, endotoxin-regulated early response gene

LPS is a gram-negative bacterial cell wall constituent also known as the endotoxin. In response to LPS exposure,

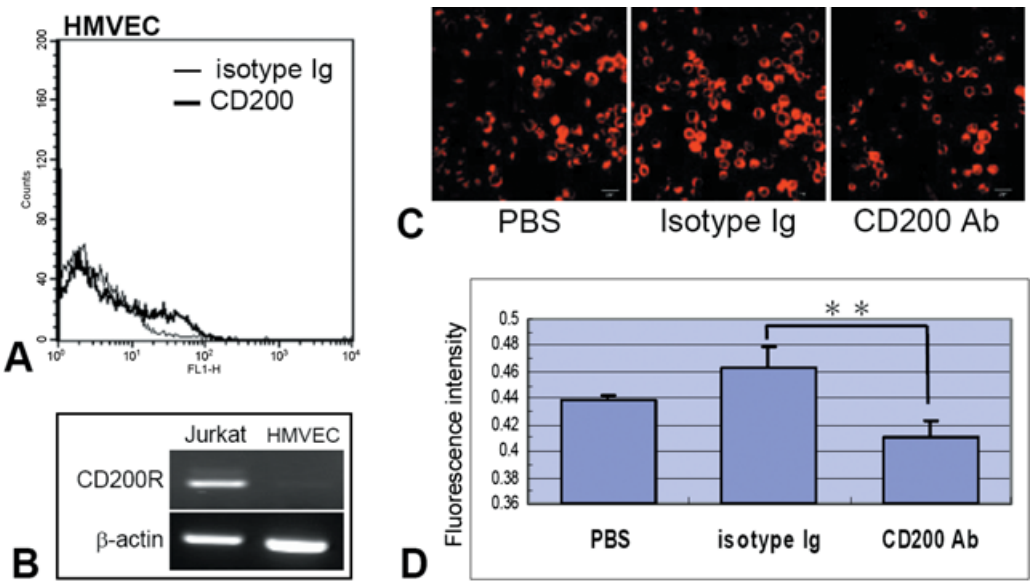

Fig. 10 Involvement of CD200–CD200R1 interaction in the adhesion of human T lymphocytic leukemia cell line (Jurkat T cells) to HMVECs. Surface expression of CD200 on a subset of HMVECs (A) is verified by flow cytometry and the expression of CD200R (CD200R1) mRNA in Jurkat T cells (B) is confirmed by RT-PCR in contrast to the lack of expression in HMVECs. Cell adhesion assay shows a decreased population of pre-labeled Jurkat T cells adhering to HMVECs after CD200 antibody treatment (C). Quantitative analysis confirms that CD200 antibody significantly blocks the adhesion of Jurkat T cells on HMVECs (D). $^{**}P = 0.009$.

vascular endothelial cells undergo changes toward an inflammatory state (Dauphinee & Karsan, 2006). Previous studies reported that production of adhesion molecules, cytokines, and nitric oxide was regulated differentially between the macrovascular and microvascular endothelial cells by LPS, TNF-α, IL-1β, and IFN-γ (Haraldsen et al. 1996; Geiger et al. 1997; Beck et al. 1999). Among them, different responsiveness of HUVECs and HMVECs to LPS has been documented (Swerlick et al. 1991). Our results are in agreement with this demonstration that macrovascular HUVECs responded more vigorously to LPS than microvascular HMVECs, which showed a slight or negligible change of CD200 expression following LPS challenge. Our study further showed a pronounced increase in CD200 expression after a 2–4-h treatment with LPS in macrovascular HUVECs and HAECs, indicating that CD200 is an early response gene under LPS regulation. There is evidence that CD200 expression was induced by ERK (Petermann et al. 2007) and regulated by transcription factors p53 and C/EBPβ (Rosenblum et al. 2004a; Chen et al. 2006). Moreover, only in HUVECs, CD200 expression was subsequently augmented after 12 h of LPS challenge. This is possibly due to a secondary response mediated by the LPS induction of inflammatory cytokine secretion such as endothelial IL-1. The provoking effect of IL-1 on CD200 expression was suggested based on the microarray analysis of HUVECs (Mayer et al. 2004). Indeed, signaling triggered by IL-1 or LPS was able to induce transcription of C/EBPβ (Lekstrom-Himes & Xanthopoulos, 1998), a transcription factor up-regulating CD200 mRNA expression (Chen et al. 2006). Our results, together with the others, suggest that endothelial cell response to LPS is cell-type specific, and it varies in the induction magnitude of an early response gene CD200.

Gram-negative bacterial infection results in septic shock in which LPS impairs the barrier function of vascular endothelium. The endothelium then undergoes inflammatory changes, featuring up-regulation of immune molecules including the adhesion molecules belonging to the IgSF, e.g. VCAM-1 and ICAM-1 (Chen et al. 1995; Kim & Koh, 2000; Zhao et al. 2001; Tseng et al. 2006). At the same time, LPS elevated the expression of certain negative immunoregulators such as spermine, IL-1 receptor antagonist, and Rbpsuh (Zhao et al. 2001; Tseng et al. 2006). These findings indicate that the overall outcome of LPS-induced immune responses is achieved by generating a shift of balance between the immunostimulatory and immunosuppressive factors. In the present results, we have provided evidence that endothelial CD200 can act as an immunosuppressive signal for macrophage adhesion and is elicited after LPS stimulation. It is therefore concluded that endothelial CD200, being an IgSF member with well known immunosuppressive activity, is involved in the homeostasis of immune responses through its preventive effect on the aberrant adhesion/diapedesis of immune cells during tissue inflammation and injuries.

Acknowledgements

We greatly appreciate Dr Leung-Kei Siu, Infectious Diseases Unit, Division of Clinical Research, National Health Research Institutes for his kind gift of HBMECs. This study was supported in part by research grants (NSC96-2320-B016-010; NSC96-2320-B006-037) from the National Science Council, Taiwan.

References

Aird WC (2003) Endothelial cell heterogeneity. *Crit Care Med* **31**, S221–230.

Aird WC (2007) Phenotypic heterogeneity of the endothelium: I. Structure, function, and mechanisms. *Circ Res* **100**, 158–173.

Alitalo K, Carmeliet P (2002) Molecular mechanisms of lymphangiogenesis in health and disease. *Cancer Cell* **1**, 219–227.

Andersson M, Karlsson L, Svensson PA, et al. (2005) Differential global gene expression response patterns of human endothelium exposed to shear stress and intraluminal pressure. *J Vasc Res* **42**, 441–452.

Barclay AN (1981) Different reticular elements in rat lymphoid tissue identified by localization of Ia, Thy-1 and MRC OX 2 antigens. *Immunology* **44**, 727–736.

Barclay AN, Ward HA (1982) Purification and chemical characterisation of membrane glycoproteins from rat thymocytes and brain, recognised by monoclonal antibody MRC OX 2. *Eur J Biochem* **129**, 447–458.

Beck GC, Yard BA, Breedijk AJ, Van Ackern K, Van Der Woude FJ (1999) Release of CXC-chemokines by human lung microvascular endothelial cells (LMVEC) compared with macrovascular umbilical vein endothelial cells. *Clin Exp Immunol* **118**, 298–303.

Bukovsky A, Presl J, Zidovsky J, Mancal P (1983) The localization of Thy-1.1, MRC OX 2 and Ia antigens in the rat ovary and fallopian tube. *Immunology* **48**, 587–596.

Chen CC, Rosenbloom CL, Anderson DC, Manning AM (1995) Selective inhibition of E-selectin, vascular cell adhesion molecule-1, and intercellular adhesion molecule-1 expression by inhibitors of I kappa B-alpha phosphorylation. *J Immunol* **155**, 3538–3545.

Chen DX, He H, Gorczynski RM (2005) Synthetic peptides from the N-terminal regions of CD200 and CD200R1 modulate immunosuppressive and anti-inflammatory effects of CD200-CD200R1 interaction. *Int Immunol* **17**, 289–296.

Chen Z, Marsden PA, Gorczynski RM (2006) Cloning and characterization of the human CD200 promoter region. *Mol Immunol* **43**, 579–587.

Cherwinski HM, Murphy CA, Joyce BL, et al. (2005) The CD200 receptor is a novel and potent regulator of murine and human mast cell function. *J Immunol* **174**, 1348–1356.

Chi JT, Chang HY, Haraldsen G, et al. (2003) Endothelial cell diversity revealed by global expression profiling. *Proc Natl Acad Sci USA* **100**, 10623–10628.

Chitnis T, Imitola J, Wang Y, et al. (2007) Elevated neuronal expression of CD200 protects Wlds mice from inflammation-mediated neurodegeneration. *Am J Pathol* **170**, 1695–1712.

Clark MJ, Gagnon J, Williams AF, Barclay AN (1985) MRC OX-2 antigen: a lymphoid/neuronal membrane glycoprotein with a structure like a single immunoglobulin light chain. *EMBO J* **4**, 113–118.

Dauphinee SM, Karsan A (2006) Lipopolysaccharide signaling in endothelial cells. *Lab Invest* **86**, 9–22.

Fallarino F, Asselin-Paturel C, Vacca C, et al. (2004) Murine plasmacytoid dendritic cells initiate the immunosuppressive pathway of tryptophan catabolism in response to CD200 receptor engagement. *J Immunol* **173**, 3748–3754.

Geiger M, Stone A, Mason SN, Oldham KT, Guice KS (1997) Differential nitric oxide production by microvascular and macrovascular endothelial cells. *Am J Physiol* **273**, L275–281.

Gorczynski L, Chen Z, Hu J, et al. (1999) Evidence that an OX-2-positive cell can inhibit the stimulation of type 1 cytokine production by bone marrow-derived B7-1 (and B7-2)-positive dendritic cells. *J Immunol* **162**, 774–781.

Gorczynski RM, Hadidi S, Yu G, Clark DA (2002) The same immunoregulatory molecules contribute to successful pregnancy and transplantation. *Am J Reprod Immunol* **48**, 18–26.

Haraldsen G, Kvale D, Lien B, Farstad IN, Brandtzaeg P (1996) Cytokine-regulated expression of E-selectin, intercellular adhesion molecule-1 (ICAM-1), and vascular cell adhesion molecule-1 (VCAM-1) in human microvascular endothelial cells. *J Immunol* **156**, 2558–2565.

Henninger DD, Panes J, Eppihimer M, et al. (1997) Cytokine-induced VCAM-1 and ICAM-1 expression in different organs of the mouse. *J Immunol* **158**, 1825–1832.

Hoek RM, Ruuls SR, Murphy CA, et al. (2000) Down-regulation of the macrophage lineage through interaction with OX2 (CD200). *Science* **290**, 1768–1771.

Ishii H, Salem HH, Bell CE, Laposata EA, Majerus PW (1986) Thrombomodulin, an endothelial anticoagulant protein, is absent from the human brain. *Blood* **67**, 362–365.

Kim H, Koh G (2000) Lipopolysaccharide activates matrix metalloproteinase-2 in endothelial cells through an NF-kappaB-dependent pathway. *Biochem Biophys Res Commun* **269**, 401–405.

Lekstrom-Himes J, Xanthopoulos KG (1998) Biological role of the CCAAT/enhancer-binding protein family of transcription factors. *J Biol Chem* **273**, 28545–28548.

Levin EG, Santell L, Osborn KG (1997) The expression of endothelial tissue plasminogen activator in vivo: a function defined by vessel size and anatomic location. *J Cell Sci* **110** (Pt 2), 139–148.

Luster AD, Alon R, von Andrian UH (2005) Immune cell migration in inflammation: present and future therapeutic targets. *Nat Immunol* **6**, 1182–1190.

Mayer H, Bilban M, Kurtev V, et al. (2004) Deciphering regulatory patterns of inflammatory gene expression from interleukin-1-stimulated human endothelial cells. *Arterioscler Thromb Vasc Biol* **24**, 1192–1198.

McMaster WR, Williams AF (1979) Identification of Ia glycoproteins in rat thymus and purification from rat spleen. *Eur J Immunol* **9**, 426–433.

Minami T, Aird WC (2005) Endothelial cell gene regulation. *Trends Cardiovasc Med* **15**, 174–184.

Miyasaka M, Tanaka T (2004) Lymphocyte trafficking across high endothelial venules: dogmas and enigmas. *Nat Rev Immunol* **4**, 360–370.

Petermann KB, Rozenberg GI, Zedek D, et al. (2007) CD200 is induced by ERK and is a potential therapeutic target in melanoma. *J Clin Invest* **117**, 3922–3929.

Pusztaszeri MP, Seelentag W, Bosman FT (2006) Immunohistochemical expression of endothelial markers CD31, CD34, von Willebrand factor, and Fli-1 in normal human tissues. *J Histochem Cytochem* **54**, 385–395.

Rao RM, Yang L, Garcia-Cardena G, Luscinskas FW (2007) Endothelial-dependent mechanisms of leukocyte recruitment to the vascular wall. *Circ Res* **101**, 234–247.

Rosenblum MD, Olasz E, Woodliff JE, et al. (2004a) CD200 is a novel p53-target gene involved in apoptosis-associated immune tolerance. *Blood* **103**, 2691–2698.

Rosenblum MD, Olasz EB, Yancey KB, et al. (2004b) Expression of CD200 on epithelial cells of the murine hair follicle: a role in tissue-specific immune tolerance? *J Invest Dermatol* **123**, 880–887.

Shiratori I, Yamaguchi M, Suzukawa M, et al. (2005) Down-regulation of basophil function by human CD200 and human herpesvirus-8 CD200. *J Immunol* **175**, 4441–4449.

Swerlick RA, Garcia-Gonzalez E, Kubota Y, Xu YL, Lawley TJ (1991) Studies of the modulation of MHC antigen and cell adhesion molecule expression on human dermal microvascular endothelial cells. *J Invest Dermatol* **97**, 190–196.

Tseng HW, Juan HF, Huang HC, et al. (2006) Lipopolysaccharide-stimulated responses in rat aortic endothelial cells by a systems biology approach. *Proteomics* **6**, 5915–5928.

Webb M, Barclay AN (1984) Localisation of the MRC OX-2 glycoprotein on the surfaces of neurones. *J Neurochem* **43**, 1061–1067.

Wright GJ, Puklavec MJ, Willis AC, et al. (2000) Lymphoid/neuronal cell surface OX2 glycoprotein recognizes a novel receptor on macrophages implicated in the control of their function. *Immunity* **13**, 233–242.

Wright GJ, Jones M, Puklavec MJ, Brown MH, Barclay AN (2001) The unusual distribution of the neuronal/lymphoid cell surface CD200 (OX2) glycoprotein is conserved in humans. *Immunology* **102**, 173–179.

Yamamoto K, de Waard V, Fearns C, Loskutoff DJ (1998) Tissue distribution and regulation of murine von Willebrand factor gene expression in vivo. *Blood* **92**, 2791–2801.

Zhao B, Bowden RA, Stavchansky SA, Bowman PD (2001) Human endothelial cell response to gram-negative lipopolysaccharide assessed with cDNA microarrays. *Am J Physiol Cell Physiol* **281**, C1587–1595.